Anticancer Activity and Molecular Mechanism of Resveratrol–Bovine Serum Albumin Nanoparticles on Subcutaneously Implanted Human Primary Ovarian Carcinoma Cells in Nude Mice

Liyuan Guo,[1] Yan Peng,[2,*] Jingping Yao,[2] Lihua Sui,[1,*] Anxin Gu,[1] and Jing Wang[1]

Abstract

This study investigates the antitumor effects and functional mechanism of resveratrol–bovine serum albumin nanoparticles (RES-BSANP) on human primary ovarian carcinoma cells in nude mice. An implanted tumor model was established by injecting a suspension of the human primary ovarian cancer cell $SKOV_3$ into the subcutaneous tissue of nude mice. The tumor-bearing mice ($n = 32$) were randomly divided into 8 groups, which received intraperitoneal injections of normal saline (0.9%, 0.5 mL), BSA (1.5 mg/kg, 0.5 mL), or RES-BSANP or RES (200, 100, and 50 mg/kg, 0.5 mL), respectively, once a week for 4 weeks. The *in vivo* antitumor efficacy was evaluated by measurement of tumor volume, whereas morphological alterations were observed by transmission electron microscope (atomic force microscopy); TUNEL assays and immunoblotting for apoptotic and cell proliferation proteins were carried out to elucidate the possible mechanism. RES-BSANP was found to exhibit certain highly desirable characteristics such as innocuity, better dispersity, and water solubility; it affected the *in vivo* tissue/organ distribution of RES in a remarkable manner. The administration of RES-BSANP significantly retarded the growth of carcinomas in nude mice from the third week onwards, and the inhibition rate was markedly higher than in mice treated with RES (52.43% vs. 46.34%, $p < 0.05$), without causing weight loss ($p > 0.05$). Simultaneously, apoptotic and necrotic morphological characteristics were observed with electron microscopy in the tumor tissues of treated mice. TUNEL staining revealed that the tumors from RES-BSANP-treated mice exhibited a similar apoptotic index as RES control tumors. Western blot analysis of the protein expression profiles revealed that part of the mechanism may be mediated by triggering the release of cytochrome *c* from the intermembrane space and upregulating the expression of caspase-9 and caspase-3, suggesting that the mitochondrial apoptotic pathway was being activated.

Key words: mitochondria, neoplasm implantation, resveratrol, resveratrol–bovine serum albumin nanoparticles
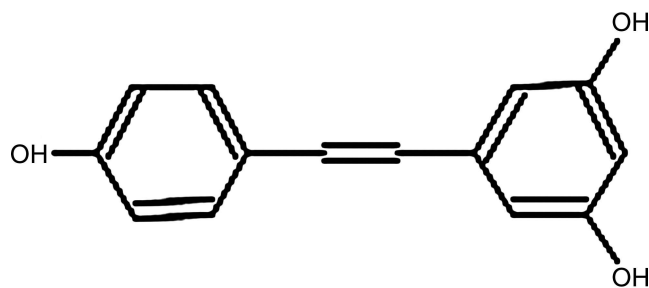
Introduction

Resveratrol (RES; see Chemical Structure) is a vegetable antitoxic agent extracted from grapes, fruits, or the roots of plants belonging to the Polygonaceae family; there is a large body of evidence on its efficacy as an antitumor agent.[1–3] However, under traditional means of administration, the absorption of RES is hampered because of its insolubility,

which limits its biological activity, both *in vitro* and *in vivo*. To solve this problem, we pioneered the synthesis of RES–bovine serum albumin nanoparticles (RES-BSANP) and reported its superior characteristics as well as enhanced antiproliferative activity on $SKOV_3$ primary cancer cells in preliminary *in vitro* experiments.[4] The present study aims to evaluate the *in vivo* potential of RES-BSANP as an anticancer agent by exploring its tissue/organ distribution, and its efficacy against the

[1]Department of Medical Oncology, Tumor Hospital of Harbin Medical University, Harbin, China.
[2]Department of Gynecology, The 1st Affiliated Hospital of Heilongjiang Chinese Traditional Medicine, Harbin, China.
*These authors equally contributed to this work.

Address correspondence to: Jing Wang; Department of Medical Oncology, Tumor Hospital of Harbin Medical University; Baojian Road 150#, Nangang District, Harbin 150086, China
E-mail: **guoliyuan80@163.com**

CHEMICAL STRUCTURE: Resveratrol.

proliferation of transplanted SKOV$_3$ cells; the study also elucidates its possible mechanism of action.

Apoptotic cell death is an active process mediated by various signaling pathways. Several studies have suggested that mitochondria play a central role in the mechanism of apoptosis.[5–6] Cytochrome c (Cyto c) is first released from the intermembrane space of the mitochondria into the cytoplasm in response to apoptotic stimuli, following which apoptotic protease activating factor-3 (APAF-3)/caspase-9, which functions as an initiator caspase, activates downstream effector caspases such as caspase-3, 8, and so on. We studied the key agents (Cyto c, caspase-9, and caspase-3) in the mitochondrial apoptosis pathway and observed the changes induced by RES[7] and RES-BSANP, to provide a theoretical and experimental basis for their possible clinical use.

Experiment

Materials

The human ovarian cancer cell strain SKOV$_3$ was obtained from the Tumor Institute of Harbin Medical University. RES was purchased from Xian Huacui Biology Co. Ltd. (purity ≥99.9%) and dissolved in dimethyl sulfoxide. RES-BSANP was prepared in the Life Science Laboratory of Northeast Forestry University. Cyto c, caspase-9, and caspase-3 monoclonal antibodies were purchased from Beijing Zhongshan Biotechnology Co. Ltd. Balb/c (nu/nu) female nude mice (4 weeks old, 18–20 g) were purchased from Beijing Wei-tong Li-hua Laboratory Animals and Technology Ltd. RES-BSANP was prepared and offered by the Life Sciences Laboratory of Northeast Forestry University. Atomic force microscope (AFM; CSPM 2000 wt) and high-performance liquid chromatography (HPLC) kit (LC-10ATVP) were obtained from Shimadzu.

Evaluation of the characteristics of RES-BSANP and HPLC analysis of drug distribution in mice

We used transmission electron microscope (AFM) and HPLC[8] to evaluate the characteristics of RES-BSANP.

Kunming mice (female, weight 18–20 g; from the Institute of Oncology of Harbin Medical University) were randomly divided into 2 groups with 5 mice in each group as follows: group 1 was designated the control group and treated with RES, and group 2 was designated the experimental group and treated with RES-BSANP. A single injection of RES or RES-BSANP (1.5 mg/kg) was delivered via the tail vein. Plasma (1.0 mL) was collected at 1, 1.5, 2, 2.5, 3, 3.5, 4,

4.5, and 5 hours postinjection and then mixed with 5 mL chloroform–methanol (1:1). Following shaking for 5 minutes, the mixture was centrifuged at 2000 rpm for 10 minutes. The chloroform layer was harvested and dried at 40°C by nitrogen gas. The remainder was dissolved in 100 μL moving phase, from which 10 μL was taken for HPLC analysis. As for the tissue samples taken from the mice liver, heart, and kidney, 1 g of each sample was homogenized in 2 mL of phosphate-buffered saline (PBS; pH = 7.90), respectively. The method was employed as mentioned above, except for substitution of the plasma with 2 mL of the homogenized mixture. Finally, 100 μL moving phase was used to dissolve the dried remainder and 10 μL was taken for HPLC analysis.

Cell and animal culture

The ovarian cancer cell line SKOV$_3$ was cultured in RPMI1640 (Gibco) supplemented with 10% heat-inactivated fetal calf serum (Gibco) in a humidified incubator at 37°C with 5% CO$_2$. Then, 2.5 g/L trypsin and 0.2 g/L ethylenediaminetetraacetic acid were used to subculture. Female BALB nu/nu mice ($n = 32$), aged 3–4 weeks, weighing 16–20 g, were bred in specific pathogen-free condition in mesh cages under controlled conditions of temperature (23°C ± 3°C) and relative humidity (50% ± 20%), with 10–15 air changes per hour and light illumination for 12 hours a day. The animals were allowed access to food and tap water *ad libitum* throughout the acclimatization and experimental periods.

Establishment of nude mice model

SKOV$_3$ cells were grown in monolayer culture, harvested, and adjusted to 5×10^6 cells/mL. For subcutaneous tumor formation, 0.2 mL of cell solution was injected subcutaneously into the right back of each nude mouse. About 7 days postimplantation, when the tumor was visible, the nude mice were randomly allocated into 8 groups with 4 mice to each group as follows: group A received normal saline (0.9%, 0.5 mL), group B received RES 200, 100, and 50 mg/kg, group C received RES-BSANP 200, 100, and 50 mg/kg, and D group received only BSA (1.5 mg/kg). Each group was treated with the same volume (0.5 mL) of intraperitoneal inclining injections on both sides in-turn per week for a total of 4 weeks. Each tumor tissue was measured with a sliding caliper for a maximal diameter (a) and a minimal diameter (b) on 7, 14, 21, 28, 35, 42, and 49 days, respectively; tumor volume was calculated using the following formula: volume $= a \times b \times b / 2$.

All animals were sacrificed by cervical decapitation at 49 days postadministration, and complete examination of abdominal cavity was performed. After the necrotic tissue and noncancerous tissues of the specimens were removed, the remaining cancerous tissues were cut into small pieces of about 1 mm^3. Inhibitory rate (IR) of tumor growth was calculated using the following formula: IR $= (1 - $ volume of experiment group/volume of control group$) \times 100\%$.

Transmission electron microscopy

Tumor samples were cut into 1 mm × 1 mm × 1 mm sections, which were fixed in 4% glutaral, immersed with Epon

821, and imbedded for 72 hours at 60°C. Cells were prepared into ultrathin sections (60 nm) and stained with uranyl acetate and lead citrate. Cell morphology was observed using a transmission electron microscope.

TUNEL assay for apoptosis detection

TUNEL staining was performed using an *in situ* apoptosis detection kit (Roche) to detect apoptosis in the tumor. TUNEL assay was performed as follows: The frozen tumor samples obtained were cut into 5-μm-thick sections and mounted on 3-aminopropyltriethoxysilane-treated slides. The slides were fixed with 4% paraformaldehyde solution and permeabilized with a solution of 0.1% Triton X-100 and 0.1% sodium citrate. After being washed twice with PBS, the sections were incubated with TUNEL reaction solution at 37°C for 60 minutes. The transforming solution (POD) was added and incubated at 37°C for 30 minutes. The slides were observed by DAB, dehydrated in graded alcohol, and covered with resin. The criterion for positive staining was that the nuclei were stained pale brown. The TUNEL-positive cells were enumerated in the four groups, using a light microscope. In each group, the positive cells in 10 high-power fields at a magnification of 400× were examined. The results of staining were analyzed and evaluated with American Image-Pro Plus software. The apoptotic index (AI) was calculated as the percentage of positive staining cells: AI = number of apoptotic cells/total number of nucleated cells.

Western blot analysis

Western blotting was used to detect the expression of Cyto *c*, caspase-9, and caspase-3 proteins. On day 49 after treatment, 1 g tumor tissue was collected from each nude mouse and homogenized. The tissues were lysed in a lysis buffer containing 50 mmol/L Tris-HCl (pH 7.5), 150 mmol/L NaCl, 0.5% deoxycholic acid, 1% NP40, 0.1% sodium dodecyl sulfate (SDS), 1 mmol/L PMSF, and 100 μg/mL leupeptin. Protein concentration was measured using a Bio-Rad colorimetric protein assay kit (Bio-Rad). A 50 μg sample of protein was separated on SDS–polyacrylamide gels and transferred onto a nitrocellulose membrane. Mouse anti-human Cyto *c* antibody (1:300), mouse anti-human caspase-9 antibody (1:200), mouse anti-human caspase-3 antibody (1:500), or mouse anti-α-tubulin antibody (1:500) was used, respectively, as the primary antibody. Horseradish peroxidase-conjugated anti-mouse antibody (1:1000) was used to probe for Cyto *c*, caspase-9, and caspase-3 or α-tubulin as the secondary antibody. The band was detected using the enhanced chemiluminescence detection system.

Statistical analysis

Measured results were expressed as mean ± standard deviation. One-way analysis of variance and *t*-test were performed with SPSS 11.0, with $p < 0.05$ considered as statistically significant.

Results

Characteristics of RES-BSANP

The morphology of nanoparticles was observed using AFM *in vitro*. Under optimum conditions, RES-BSANP

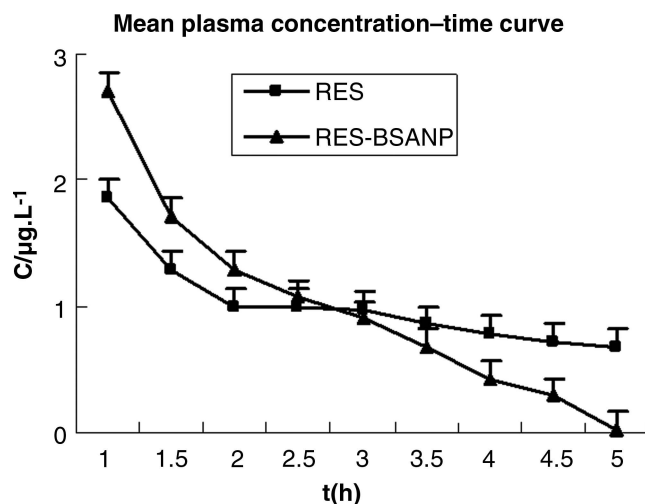**Mean plasma concentration–time curve**

FIG. 1. Mean plasma concentration–time curve of RES and RES-BSANP after injecting at different points. RES-BSANP, resveratrol–bovine serum albumin nanoparticles.

nanoparticles were smooth and round in appearance and dispersed well. The mean diameter of the nanoparticles ranged from 400 to 500 nm; the concentration of supernate was 1.585 mg/mL and the content of RES in the supernate was 7.923 mg, so the content of RES in the nanoparticles was 12 − 7.923 mg = 4.077 mg. The entrapment efficiency was calculated at 33.97 (4.077/12×100%). The maximum water solubility was enhanced 12 times, from 0.0169 to 0.2021 mg/mL. The sample solution was injected at 0, 2, 4, 6, 8, 12, and 24 hours and the scores of peak area were recorded. An RSD of 0.75% indicated the stability of RES-BSANP, whereas the suspension showed lasting stability after 1 month at room temperature. All the above data were presented in our earlier study.[4]

Tissue distribution of RES-BSANP in vivo

The present study demonstrated that compared with RES solution, RES-BSANP significantly alters its pharmacokinetics in mice, as seen in the plasma concentration–time curves of RES and RES-BSANP (Fig. 1). The results indicated that
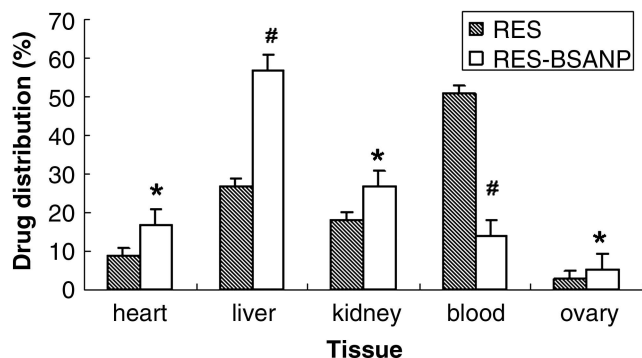

FIG. 2. The high-performance liquid chromatography analysis of tissue distribution of RES versus RES-BSANP at 4 hours after drug injection. [#]$p < 0.01$, versus RES group; *$p < 0.05$, versus RES group. RES-BSANP, resveratrol–bovine serum albumin nanoparticles.
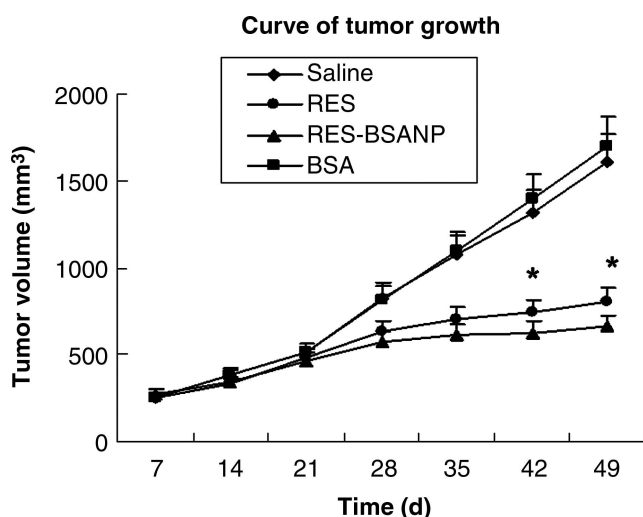
Curve of tumor growth

FIG. 3. Tumor growth curve at different marking points. *$p < 0.05$. RES-BSANP, resveratrol–bovine serum albumin nanoparticles.

the RES concentration in the large organs in group 2 (RES-BSANP injection) was significantly higher than that in group 1 (RES injection). The relative uptake efficiency was 6.063; the maximum concentration was enhanced 2.11 times, whereas the targeting efficiency to the organs was also higher (from 27.13% to 57.47%) upon treatment with RES-BSANP. These results suggested that RES-BSANP injection changed the distribution profile of RES in tissues/organs and greatly increased the concentration of drug in the liver ($p < 0.01$), kidney, heart, and ovaries ($p < 0.05$), whereas in blood, the concentration of RES-BSANP was much lower than RES ($p < 0.01$) (Fig. 2).

IR of tumor growth

All models of nude mice with transplanted ovarian carcinoma were established at 7 days after subcutaneous injection, with an average volume of 340 mm³. The rate of subcutaneous tumor formation was 100%.

Tumor growth curve at different time points showed a tendency toward slower growth in the therapeutic groups compared with the saline group. As can be seen in Figure 3, the IR of tumor growth increased sharply in the RES-BSANP-high dose (H) group compared with the RES-H group at 42 and 49 days ($p < 0.05$).

We examined whether treatment with RES-BSANP could inhibit the growth of SKOV$_3$-implanted tumors. As shown in Table 1, the growth of tumor was markedly attenuated by the treatment with RES and RES-BSANP; on the contrary, tumor growth was not significantly retarded in the normal saline group ($p < 0.05$). There were no significant differences in average tumor weight in the middle dose groups for RES and RES-BSANP ($p > 0.05$), whereas tumors in the RES-BSANP-H and RES-BSANP-low dose groups were smaller ($p < 0.05$) (Table 2).

Morphological changes

The cells in the control groups displayed normal structures, but some cells in the therapeutic groups had apoptotic characteristics including chromatin condensation, chromatin crescent, nuclear fragmentation, apoptotic bodies, and so on. On the contrary, some cells presented necrotic morphologic changes, such as degeneration of cytoplasm and molten cell nucleus (Fig. 4A–C Figure 4).

TUNEL assay for the apoptosis of tumor tissue

To elucidate the possible mechanism, we examined by immunohistochemical TUNEL analysis whether tumor growth suppression by RES-BSANP was caused by tumor cell apoptosis. Apoptotic bodies in tumor sections from control and experimental mice were observed by TUNEL staining and representative micrographs are shown in Figure 5. The tumors from RES-BSANP-treated mice presented a markedly higher count of brown-colored apoptotic bodies compared with tumors from BSA- and saline-treated controls ($p < 0.01$) and also presented a profile similar to the RES group ($p > 0.05$) as shown in Figure 6. The incidence of tumor apoptosis was not directly correlated with higher inhibition of tumor growth, suggesting that RES-BSANP caused tumor suppression by augmenting apoptosis with necrosis and/or other death pathways in the tumor.

Expression of Cyto-c, caspase-9, and caspase-3 proteins

We further investigated the pathway for apoptotic effects of RES-BSANP *in vivo*. The total proteins from the control and experiment groups' tumors were resolved by SDS–polyacrylamide gel electrophoresis and immunoblotted with specific antibodies against Cyto *c*, caspase-9, and caspase-3 molecules, which play key roles in cell apoptosis. The relative density of each band was scanned and expressed relative

TABLE 1. EFFECT OF RESVERATROL–BOVINE SERUM ALBUMIN NANOPARTICLES ON THE WEIGHTS OF NUDE MICE AND THEIR SUBCUTANEOUSLY TRANSPLANTED TUMORS ($N = 4$, MEAN ± STANDARD DEVIATION)

Group	Saline control	BSA control	RES-BSANP 50 μmol/L	RES-BSANP 100 μmol/L	RES-BSANP 200 μmol/L
Tumor weight/g	0.82 ± 0.11	0.88 ± 0.21	$0.55 \pm 0.05^*$	$0.51 \pm 0.14^{*,**}$	$0.39 \pm 0.05^{*,**}$
Mouse weight less tumor/g	17.46 ± 0.08	18.22 ± 0.18	19.05 ± 0.22	20.13 ± 0.12	20.23 ± 0.14
Mouse weight/g	24.22 ± 0.23	23.45 ± 0.17	23.22 ± 0.19	24.33 ± 0.07	23.27 ± 0.14

*$p < 0.01$ versus saline control.
**$p < 0.05$ versus BSA control.
BSA, bovine serum albumin; RES-BSANP, resveratrol–BSA nanoparticles.

TABLE 2. TUMOR WEIGHT AND INHIBITION RATE OF NUDE MOUSE AFTER EXECUTION BETWEEN TWO HIGH-DOSE GROUPS ($N = 4$, MEAN ± STANDARD DEVIATION)

Groups	Tumor weight (g) $\bar{x} \pm s$	IR (%)
Saline control	0.82 ± 0.11	
BSA control	0.88 ± 0.21	
RES-H	0.44 ± 0.07*	46.34
RES-BSANP-H	0.39 ± 0.07**	61.72
RES-M	0.47 ± 0.12*	53.28
RES-BSANP-M	0.51 ± 0.14*	52.43
RES-L	0.67 ± 0.07	43.22
RES-BSANP-L	0.59 ± 0.05*	45.27

*$p < 0.05$ versus saline control.
**$p < 0.05$ versus RES control.
IR, inhibition rate; BSA, bovine serum albumin; RES-BSANP, resveratrol–BSA nanoparticles; H, high dose; M, medium dose; L, low dose.

to α-tubulin. As shown in Figure 7, the expression of Cyto *c*, caspase-9, and caspase-3 was significantly upregulated in the B and C treatment groups, when compared with group A ($p < 0.05$); however, there were no significant differences in the expression of the three proteins among the two treatment groups ($p > 0.05$). The expression of the proteins was further semiquantified by image analysis.

Discussion

Ovarian carcinoma has a very poor prognosis with <30% 5-year survival rates and lack of effective drugs for treatment. Currently, only a few chemotherapeutic drugs are effective in the treatment of primary ovarian carcinomas and it is necessary to search for new anti-ovarian carcinoma drugs. Several studies have shown that RES has antitumor and apoptosis-inducing effects. Modern scientific research has revealed a wide variety of dietary and medicinal functions for RES, particularly growth inhibition in a wide variety of tumor cells, including leukemia, prostate, breast, and hepatic cells, and so on.[9–11] Here, we study RES as the model drug in an optimized dosage form designed to elevate its bioactivity for clinical application.

Since the introduction of nanoparticles in the early 80s, scientists have conducted a lot of research in its preparation, stability, distribution, and targeting. Recently, many scholars have attempted to make various forms of RES with different carriers,[12] and many capsules and injections are in the market; however, these hold many disadvantages such as short half-life, side-effects, and drug tolerance. Recently, more and more BSANPs such as BSANPs containing paclitaxel[13–14] have entered the horizon of antitumor treatment. With the merit of being nontoxic, safe, and economical and also possessing good biocompatibility and no immunogenicity, many studies have explored BSA as a drug carrier.[15–16] The technique for preparation of RES-BSANP is simple and has not been reported earlier. However, further studies on its characteristics, such as delayed release, are required to enhance this nanoparticle drug-delivery system and present a new chemotherapeutic drug for the treatment of ovarian cancer.

On studying its biodistribution, we discovered that there remains a large amount of RES in the blood at 1, 1.5, 2, 2.5, 3, 3.5, 4, 4.5, and 5 hours after the administration. This illustrates that the distribution of RES is incomplete because RES exists in the suspension like a cloudy polymer, but not monodispersion, and its large diameter makes absorption and distribution in target organs difficult. Our results suggested that RES-BSANP injection changed the tissue/organ distribution profile for RES *in vivo* and greatly increased the concentration of the drug in the liver. This enhanced distribution of RES in the ovary might increase its anti-oophoroma ability, which makes it possible to change the formulation for treatment and ameliorate its bioactivity. As the first report on RES-BSANP, this study represents a great achievement for
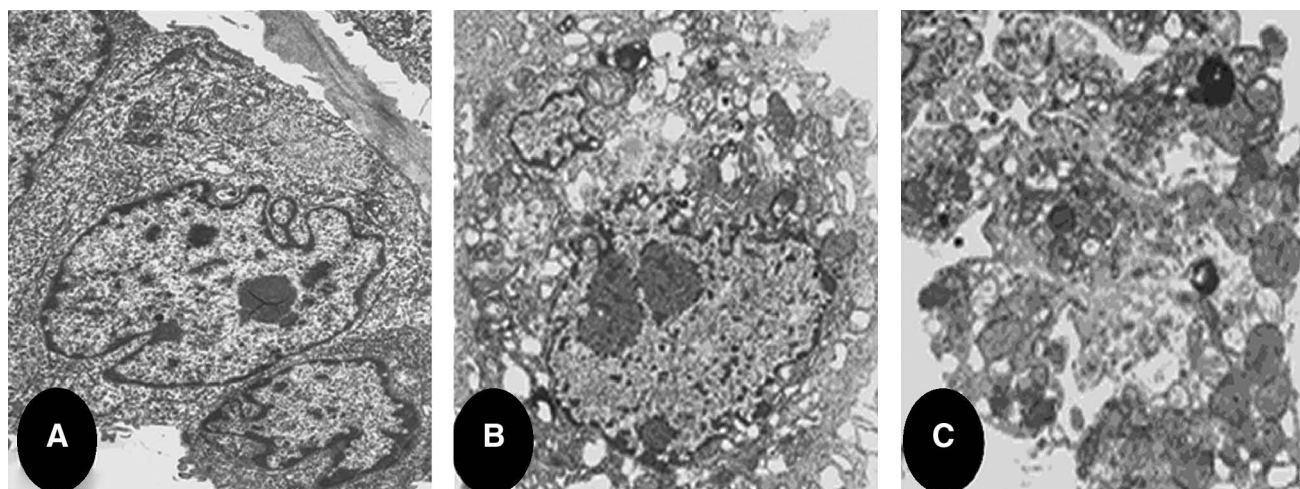

FIG. 4. Transmission electron micrograph of tumor tissue. (**A**) Saline control; (**B**) RES-H control; (**C**) RES-BSANP-H. (**A**) Abundant mitochondria and rough endoplasmic reticulum in cytoplasm, more in cell junctions. (**B**) Mitochondria karyopyknosis, remaining in cell junctions; chromatin condensation; metaphase of apoptosis. (**C**) Vacuolar degeneration of mitochondria, either apoptotic body or necrotic changes can be seen simultaneously. RES-BSANP, resveratrol–bovine serum albumin nanoparticles.
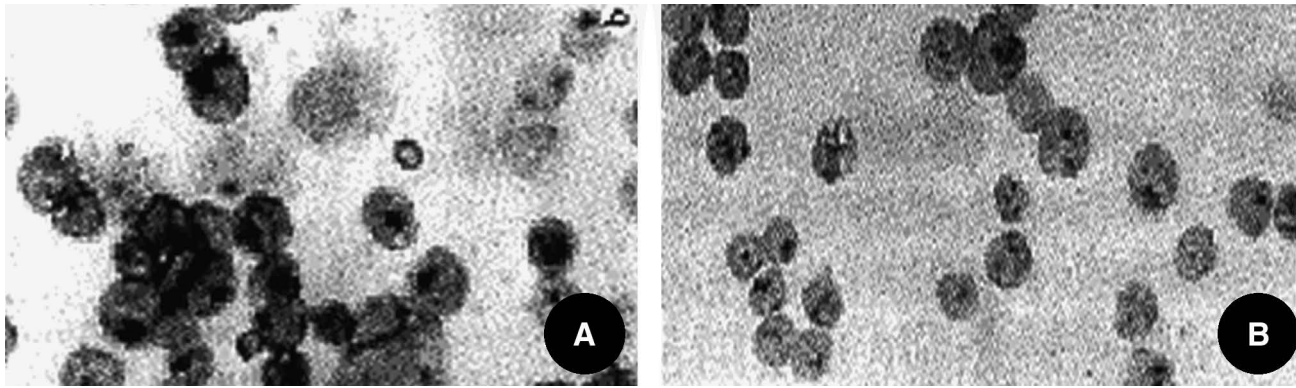
FIG. 5. TUNEL staining for apoptotic bodies in SKOV$_3$ tumor sections from RES-SABNP-treated mice and the controls (TUNEL-positive cells were dark brown). The tumors from RES-SABNP-treated mice (**A**: Group 4, original magnification ×400) exhibited a similar count of brown-color apoptotic bodies compared with RES tumors (**B**: Group 1, original magnification ×400). RES-BSANP, resveratrol–bovine serum albumin nanoparticles.

nanoparticle-based drug-delivery systems and opens a new approach for the treatment of ovarian cancer.

Subcutaneous tumor implantation has been used as a standard method to establish animal models of human cancer.[17] Although such models help understand the nature of human cancers and their therapeutic approaches, many problems remain unsolved, such as chemical peritonitis resulting from continuous intraperitoneal injection. In our previous experiments, we found some individual mice were sick with chemical intestinal obstruction. So we chose to administer inclining intraperitoneal injections, alternating between both sides in turn, which partly lessened the intestinal obstruction, as confirmed by dissection. The results indicated that this model in nude mice mimicked the natural biological behavior of human ovarian cancer. In both treatment groups, the characteristics of cell apoptosis were seen in the two high-dose treatment groups, whereas in the RES-BSANP-H group, necrosis was observed as well. These morphological changes, taken together, suggest that RES-

BSANP reduced tumor growth by triggering the necrosis of ovarian cancer cells *in vivo*, as well as stimulating the induction of cell apoptosis. TUNEL staining showed that the tumors from RES-BSANP-treated mice exhibited a similar AI compared with RES control tumors, that is, the enhanced efficiency of high-dose RES-BSANP treatment possibly arose from necrosis and/or other death pathway. Many studies have reported that with the higher drug concentration or more intensive stimuli, tumors turn to necrosis rather than apoptosis.[18] But no precise answers were available at this time. Further studies are required to elucidate the exact mechanisms involved these findings.

Many pathways and proteins control the apoptotic machinery. Many pro-apoptotic signals converge at the mitochondria, and most, if not all, of these stimuli trigger a change of the mitochondrial membrane permeability and subsequent release of mitochondrial proteins into the cytoplasm, which constitutes the key event of mitochondria-mediated apoptosis. The pro-apoptotic proteins include Cyto *c*, caspase-9, Smac\AIF, and so on. Cyto *c* is localized in the mitochondrial intermembrane space, and increased permeability of the outer mitochondrial membrane permits the
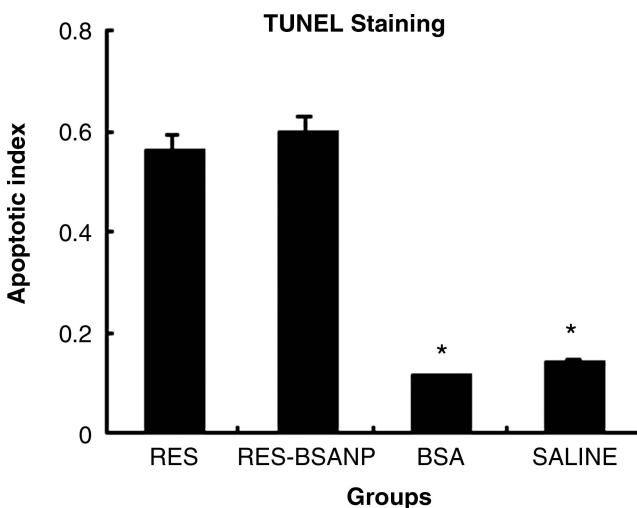

FIG. 6. TUNEL-positive cells were counted to record the apoptotic index. *$p < 0.01$, versus the control BSA and saline group. RES-BSANP, resveratrol–bovine serum albumin nanoparticles.
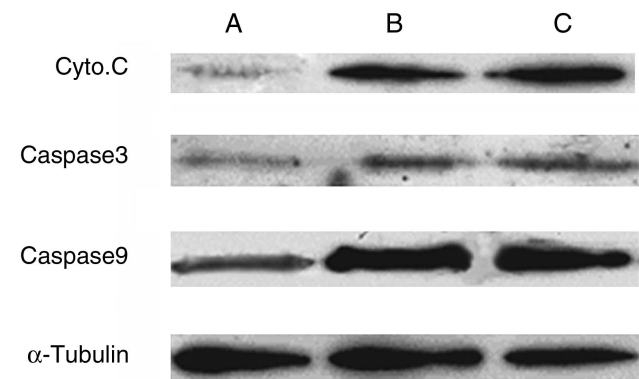

FIG. 7. Expression of the GAP-associated protein in mitochondrial apoptotic pathway. (**A**) Saline control; (**B**) RES-H control; (**C**) RES-BSANP-H group. RES-BSANP-H, resveratrol–bovine serum albumin nanoparticles-high dose.

release of Cyto *c* into the cytoplasm. Cyto *c* initiates the formation of a multiprotein complex composed of APAF-1, dATP, and caspase-9, followed by downstream effectors caspases, such as caspase-3, which spearheads the common pathway in endogenous and ectogenous apoptosis. We observed the inhibitory effect of RES in all therapeutic groups: cells in the control groups presented normal morphology, whereas cells in the therapeutic groups took on apoptotic and necrotic characteristics; the expression levels of Cyto *c*, caspase-9, and caspase-3 proteins in all therapeutic groups at the dose of 200 mg/kg were dramatically increased over those in the control group ($p < 0.05$). Our experiments demonstrated that the levels of protein expression for these proteins in tumor tissue clearly correlated with the suppression of tumor growth. We propose that caspase-related proteins orchestrate the *in vivo* tumor suppression mediated by RES-BSANP. Further studies are required to elucidate the exact mechanisms involved.

Conclusions

To summarize, we report that RES-BSANP can cause tumor inhibition in a mouse model; however, the mechanisms by which these highly promising cancer chemopreventive agents act remain elusive and need further study.

Acknowledgments

Disclosure Statement

No conflicts of interest are reported for any of the authors.

References

1. Sengottuvelan M, Deeptha K, Nalini N. Influence of dietary resveratrol on early and late molecular markers of 1, 2-dimethylhydrazine-induced colon carcinogenesis. Nutrition 2009;25:1169.
2. Bhat KP, Pezzuto JM. Cancer chemopreventive activity of resveratrol. Ann NY Acad Sci 2002;957:210.
3. Kuwajerwala N, Cifuentes E, Gautam S. Resveratrol induces prostate cancer cell entry into s phase and inhibits DNA synthesis. Cancer Res 2002;62:2488.
4. Guo L-Y, Yao J-P, Sui L-H. Preparation and effects of resveratrol bovine serum albumin nanoparticles on proliferation of human ovarian carcinoma cell SKOV3. Chem J Chin Univ 2009;30:474.
5. Mignotte B, Vayssiere JL. Mitochondria and apoptosis. Eur J Biochem 1998;252:1.
6. Pavlov EV, Prault M, Pietkiewicz D, et al. A novel, high conductance channel of mitochondria linked to apoptosis in mammalian cells and Bax expression in yeast. J Cell Biol 2001;155:725.
7. Dorrie J, Geraucer H, Wachter Y, et al. Resveratrol induces extensive apoptosis by depolarizing mitochondrial membranes and activating caspase-9 in acute lymphoblastic leukemia cells. Cancer Res 2001;61:4731.
8. Bobbin RP, Ceasar G, Fallon M. Potassium induced release of GABA and other substances from the guinea pig cochlea. Hear Res 1990;46:83.
9. Chen J, Dong X-S, Guo X-G. Functional mechanism of resveratrol in inhabiting growth of cells ls174t and its mechanism in subcutaneously transplanted tumor of nude mice. Res Chin Univ 2008;24:1.
10. Filomeni G, Graziani I, Rotilio G. Trans-resveratrol induces apoptosis in human breast cancer cells MCF-7 by the activation of MAP kinases pathways. Genes Nutr 2007;2:295.
11. Cardile V, Scifo C, Russo A, et al. Involvement of HSP70 in resveratrol-induced apoptosis of human prostate cancer. Anticancer Res 2003;23:4921.
12. Gao X-C. The use of the bovine serum albumin. Mod J Integr Tradit Chin West Med 2004;13:918.
13. Wang X-C, Hou S-X. Optimized formulation of resveratrol solid lipid nanoparticles by uniform design in combination with central composite design/response surface methodology. Chin Tradit Pat Med 2007;8:203.
14. Muller-Goymann CC. Physicochemical characterisation of colloidal drug delivery systems such as reverse micelles, vesicles, liquid crystals and nanoparticles for topical administration (invited review). Eur J Pharm Biopharm 2004; 58:343.
15. Arnedo A, Espuelas S, Irache JM. Albumin nanoparticles as carriers for a phosphodiester oligonucleotide. Int J Pharm 2002;244:59.
16. Arnedo A, Irache JM, Merodio M, et al. Albumin nanoparticles improved the stability, nuclear accumulation and anticytomegaloviral activity of aphosphodiester oligonucleotide. J Controlled Release 2004;94:217.
17. Fidler IJ. Critical factors in the biology of human cancer metastasis: Twenty-eighth GHA. Clowes memorial award lecture. Cancer Res 1990;50:6130.
18. Ramirez-Ortega M, Maldonado-Lagunas V, Melendez-Zajgla J, et al. Proliferation and apoptosis of HeLa cells induced by *in vitro* stimulation with digitalis. Eur J Pharmacol 2006;534:71.